Bed Agglomeration Characteristics in Fluidized Quartz Bed Combustion of Phosphorus-Rich Biomass Fuels

ARTICLE *in* ENERGY & FUELS · FEBRUARY 2011

Impact Factor: 2.79 · DOI: 10.1021/ef101451e

4 AUTHORS:

Alejandro Grimm
Swedish University of Agricultural Sciences
17 PUBLICATIONS **412** CITATIONS
SEE PROFILE

Nils Skoglund
Luleå University of Technology
10 PUBLICATIONS **169** CITATIONS
SEE PROFILE

Dan Boström
Umeå University
136 PUBLICATIONS **1,980** CITATIONS
SEE PROFILE

Marcus Öhman
Luleå University of Technology
86 PUBLICATIONS **1,987** CITATIONS
SEE PROFILE

energy&fuels

ARTICLE

pubs.acs.org/EF

Bed Agglomeration Characteristics in Fluidized Quartz Bed Combustion of Phosphorus-Rich Biomass Fuels

Alejandro Grimm,*[,†] Nils Skoglund,[‡] Dan Boström,[‡] and Marcus Öhman[†]

[†]Energy Engineering, Department of Engineering Sciences & Mathematics, Luleå University of Technology, SE-971 87 Luleå, Sweden

[‡]Energy Technology and Thermal Process Chemistry, Umeå University, SE-901 87 Umeå, Sweden

ABSTRACT: The bed agglomeration characteristics during combustion of phosphorus-rich biomass fuels and fuel mixtures were determined in a fluidized (quartz) bed reactor (5 kW). The fuels studied (separately and in mixtures) included logging residues, bark, willow, wheat straw, and phosphorus-rich fuels, like rapeseed meal (RM) and wheat distillers dried grain with solubles (DDGS). Phosphoric acid was used as a fuel additive. Bed material samples and agglomerates were studied by means of scanning electron microscopy (SEM) in combination with energy-dispersive X-ray spectroscopy (EDX), in order to analyze the morphological and compositional changes of coating/reaction layers and necks between agglomerated bed particles. Furthermore, bed ash particles were separated by sieving from the bed material samples and analyzed with SEM/EDS and powder X-ray diffraction (XRD). For logging residues, bark, and willow, with fuel ash rich in Ca and K but with low contents of P and organically bound Si, the bed layer formation is initiated by reactions of gaseous or liquid K compounds with the surface of the bed material grains, resulting in the formation of a potassium silicate melt. The last process is accompanied by the diffusion/dissolving of Ca into the melt and consequent viscous flow sintering and agglomeration. The addition of high enough phosphorus content to convert the available fuel ash basic oxides into phosphates reduced the amount of K available for the reaction with the quartz bed material grains, thus preventing the formation of an inner bed particle layer in the combustion of logging residues, bark, and willow. Some of the phosphate-rich ash particles, formed during the fuel conversion, adhered and reacted with the bed material grains to form noncontinuous phosphate−silicate coating layers, which were found responsible for the agglomeration process. Adding phosphorus-rich fuels/additives to fuels rich in K and Si (e.g., wheat straw) leads to the formation of alkali-rich phosphate−silicate ash particles that also adhered to the bed particles and caused agglomeration. The melting behavior of the bed particle layers/coatings formed during combustion of phosphorus-rich fuels and fuel mixtures is an important controlling factor behind the agglomeration tendency of the fuel and is heavily dependent on the content of alkaline earth metals in the fuel. A general observation is that phosphorus is the controlling element in ash transformation reactions during biomass combustion in fluidized quartz beds because of the high stability of phosphate compounds.

1. INTRODUCTION

Utilization of biomass as largely available low cost renewable and CO_2-neutral source of energy is continuously increasing. Combustion is an attractive and also a relatively mature technology for biomass utilization. Because of the inherent advantages of low process temperatures, flexibility, and emission control, fluidized bed reactors are particularly suitable for biomass combustion. However, bed agglomeration could be a potential problem, which in the most severe cases can lead to bed defluidization and unscheduled plant shut down.

Extensive research has been done regarding the employment of high alkali biomass fuels in fluidized bed combustion.[1−4] Bed agglomeration phenomenon in the fluidized bed combustion of low phosphorus biomass fuels has been a subject of several studies, and its understanding is fairly good, if not complete. The initiation of the agglomeration/defluidization process has been associated to the formation of low-temperature melting ash compounds and/or layers on the surface of the bed material grains.[5−10]

The chemical composition of the bed particle layers has been shown to have strong dependence on the fuel ash and bed material composition. Furthermore, the bed particle layer may consist of several superimposed layers with different properties and composition.[10−13] Inner layers seem to be more dependent on the bed material composition, and outer layers have a composition that is more similar to the fuel ash characteristics.[6,10,14,15]

The different dominating mechanisms behind the bed particle layer formation and bed agglomeration for nonphosphorus-rich biomass fuels in quartz beds were summarized by Brus et al.[2,10] and later updated by De Geyter et al.[15] They included the following: (a) bed layer formation initiated by potassium silicate melt (formed on the bed particle surfaces by the reaction with gaseous or liquid K compounds) accompanied by diffusion/dissolving of Ca into the melt, followed by viscous flow sintering and agglomeration (typical for woody fuels containing Ca, K, and relatively low amounts of Si), (b) direct reactions of K compounds in gaseous or aerosol phases with bed particle surfaces, forming low melting K silicate layers with subsequent development of viscous flow sintering and agglomeration (typical for fuels with high alkali and relatively low silicon content), (c) direct adhesion of bed particles by partly molten ash-derived potassium

Received: October 23, 2010
Revised: January 13, 2011
Published: February 20, 2011

silicate particles/droplets (typical for fuels with high potassium and organically bound Si, i.e., Si that is integrated (on a molecular level) in the organic structure of the biomass, and low content of other ash-forming elements). The bed material plays an active role in the agglomeration processes dominated by mechanisms (a) and (b) but to a much lesser extent in (c) because of limited interactions between the ash-forming compounds and the bed material.

During the recent decades, most of the research on fluidized bed combustion regarding the bed agglomeration problem has been focused on biomasses with low phosphorus content. However, the ash-forming matter in some agricultural biomasses or residues from production of, for example, biodiesel or bioethanol is rather different in comparison to woody biomass and various straws. The main difference is the much higher content of phosphorus, which has major influence on the ash transformation reactions.[16−20]

Relatively little research regarding bed agglomeration characteristics/mechanisms during combustion or gasification of phosphorus-rich biomasses could be found in the literature.[19−24] Boström et al., employing different mixtures of bark and rapeseed meal (RM) observed clear differences in the bed agglomeration characteristics between phosphorus-rich and phosphorus-poor biomass fuels and fuel mixtures. The quartz bed grains with continuous inner reaction layers, observed in fluidized bed combustion of woody biomass fuels, were not seen when the fuel (bark) was co-fired with the rapeseed meal containing high concentration of phosphorus. Instead, discontinuous and thin coating ash layers were observed together with isolated partially molten ash particles. The bed agglomeration mechanism proposed by the authors for the phosphorus-rich fuel mixtures involved the adhesion of bed particles by partially molten ash-derived potassium−calcium phosphates. On the other hand, for the woody fuel, bed agglomeration involved the direct reaction of gaseous alkali with the bed particles forming potassium−calcium silicate-rich bed grain layers.[19] Piotrowska and co-authors also found agglomerate necks consisting mainly of potassium, calcium, and phosphorus in co-combustion of rapeseed cake and wood.[20] Barišić and co-authors found that the addition of limestone to the mixtures of rapeseed cake and wood prevented bed agglomeration because of the formation of bed particle coatings containing high-temperature melting phosphates.[21] During full scale combustion of wood and grain waste (oat seed) in a 75 MW_{th} BFB boiler, Silvennoinen and Hedman showed that the formed bed particle layers consisted mainly of P, K, Ca, and Mg.[22] In another study, Fryda et al., co-fired meat and bone meal (MBM) with olive bagasse residues and concluded that the phosphorus in the MBM contributed to the rapid bed agglomeration. This was explained by the formation of low-temperature melting potassium phosphates.[23] In addition, Shao and co-workers reported that alkali phosphates (KPO_3 and $NaPO_3$) and the eutectics of Fe_2O_3 and SiO_2 may play an important role in the bed defluidization process by forming compounds with low melting temperature during fluidized bed combustion of sewage sludge.[24]

However, a precise and quantitative evaluation of the role of phosphorus on the bed agglomeration process during fluidized (quartz) bed combustion of phosphorus-rich biomass fuels/fuel mixtures has not yet been presented. The main objective in the present work was therefore to determine the bed agglomeration characteristics and ash transformations mechanisms in fluidized (quartz) bed combustion of several phosphorus-rich biomass fuels/fuel mixtures.

2. MATERIALS AND METHODS

2.1. Bed Material, Fuels, and Additives. Fluidized bed combustion experiments were performed using quartz sand (>98% SiO_2) as bed material with a grain size fraction between 200 and 250 μm. A total of 13 combustion experiments were performed. Logging residues from SCA Skog AB Norrbränslen, bark that was obtained as pellets from a pellet mill in Mönsterås (Södra Skogsenergi), and willow harvested from an experimental plantation in the Institution of Agricultural Research for Northern Sweden (NJV) in Umeå were used to represent woody fuels, which typically have Ca, K, and Si as main ash-forming elements and follow bed agglomeration mechanism (a). Typical wheat straw from southern Sweden was used to represent agricultural residues with high K and Si content following agglomeration mechanism (c). Residues from ethanol production, wheat distillers dried grain with solubles (DDGS) from an ethanol producer in northern Europe, and a typical European rapeseed meal from the Karlshamn plant in southern Sweden (which mainly utilize rapeseeds from southern Sweden, Germany, and Poland), were used as P- and K-rich fuels. The DDGS and the rapeseed meal were both pelletized separately and co-pelletized with the above-mentioned raw materials. Furthermore, phosphoric acid (PA) 85% from Merck was employed as a "clean" phosphorus additive to study the influence of phosphorus on the bed agglomeration mechanisms. The reason for choosing phosphoric acid as an additive was to compare the co-fired P-rich fuels with a P additive that is likely to be much more reactive. This is important in order to get a more thorough understanding of the ash transformation reactions in combustion of phosphorus-rich fuels.

To obtain good distribution and contact between the fuel materials and the additive, fuel/additive mixtures were completed in small 20 kg batches and subsequently pelletized to a diameter of 8 mm in a laboratory scale pellet press. The fuel moisture content was 10−12%. The following mixtures were produced and combusted. DDGS was added in the amount of 40% wt d.s. to logging residues, 50% wt d.s. to willow, and 50% wt d.s. to wheat straw. Phosphoric acid (PA) was added to the logging residues at two levels, increasing the molar relation between potassium and phosphorus (P/K) in the fuel ash from 0.34 to 0.5 (PA-low) and to 0.9 (PA-high). Wheat straw was also mixed with phosphoric acid, increasing the P/K molar ratio from 0.13 to 0.5 compared to that of the pure fuel. Becasue it was problematic to obtain pellets with sufficient durability (i.e., mechanical strength/density) from pure rapeseed meal, cutter shavings were admixed to improve the pellets quality. The admixture of cutter shavings was estimated to be 20% wt d.s., by measuring the ash content of the produced pellets. The ash composition of the resulting pellets was dominated by the rapeseed meal (99% of the ash) because the ash content of the rapeseed meal and cutter shavings was 7.4 and 0.3% wt d.s., respectively. Therefore, the fuel containing 80% wt d.s. and 20% wt d.s. cutter shavings will hereafter be denoted as rapeseed meal (RM) pellets. Also bark pellets were ground and co-pelletized as described above with the pure rapeseed meal in 30% wt d. s.[19]

The employed raw materials presented in Table 1 were analyzed for the contents of ash (SS − 18 71 71), sulfur (SS − 18 71 77), chlorine (SS − 18 71 54), and main ash-forming elements (ICP-AES). The ash compositions of the sample mixtures were calculated from the compositions of the raw materials compositions (Table 2).

Table 1. Total Ash Content and the Content of Main Ash-forming Elements in the Used Raw Materials[a]

	logging residues[b]	bark[b,c]	willow[b]	wheat straw[b]	rapeseed meal[c]	DDGS[b]
ash	2.4	3.7	2.1	5.7	7.4	4.4
Si	0.29	0.50	0.086	0.80	0.09	0.101
Al	0.036	0.087	0.017	0.006	0.013	0.0013
Ca	0.51	0.743	0.50	0.40	0.721	0.109
Fe	0.024	0.042	0.01	0.005	0.034	0.01
K	0.17	0.190	0.25	1.25	1.32	1.06
Mg	0.061	0.064	0.044	0.10	0.535	0.278
Na	0.014	0.032	0.011	0.03	0.013	0.01
P	0.046	0.037	0.059	0.13	1.257	0.825
S	0.041	0.04	0.04	0.19	0.91	1.03
Cl	<0.01	0.02	<0.01	0.26	0.03	0.22

[a] Values given in weight percent of dry substance. [b] Equal to the composition of the produced pellets. [c] From Boström et al.[19]

2.2. Controlled Bench-Scale Fluidized Combustion Procedure. The experiments were conducted in a bench-scale (5 kW) bubbling fluidized bed reactor (BFB), previously described in detail by Öhman and Nordin.[25] The reactor is 2.4 m high with a fluidized bed and freeboard section diameters of 100 and 220 mm, respectively. A perforated stainless steel plate at the bottom of the fluidized bed with 1% open area is used as an air distributor. During the combustion phase, the fluidization velocity was kept 10 times higher than the minimum fluidization velocity, corresponding to about 1 m/s.

A total amount of 5 kg of each fuel was combusted in 540 g of quartz sand for 8 h or until agglomeration occurred. The bed temperature was kept at approximately 800 °C for all fuels, except for the wheat straw mixtures that were combusted at an average bed temperature of 730 °C to minimize the risk for direct agglomeration during the combustion stage. Constant temperature along the reactor was achieved with the use of preheated primary air, heat from the combustion, and electrical heaters in the freeboard section. The excess oxygen level during the experiments was approximately 8% in dry flue gas for all the experiments.

After 8 h of combustion, the fuel feeding was stopped and bed material samples were taken. Next, temperature staging was started by external heating via the wall heaters. Combustion of propane gas in a chamber prior to the primary air distributor plate was started to maintain a combustion atmosphere in the reactor, while the bed was continuously isothermally heated at 3 °C/min until bed agglomeration was achieved. The onset of defluidization is indicated by a drop in differential bed pressures, and deviations in the bed temperature measurements registered continuously. The reproducibility of the initial defluidization temperature measured with this method has previously been determined to be ±5 °C.[25]

2.3. Chemical Characterization of Bed Samples. The bed samples taken at the end of the combustion period (8 h) prior to the temperature staging phase as well as after the agglomeration test were mounted in epoxy and dry polished in order to avoid possible leach out of soluble ash elements. The cross sections of the samples were then analyzed semiquantitatively by using a Philips model XL30 scanning electron microscope (SEM) combined with an energy-dispersive X-ray spectrometer (EDS) for the determination of the morphology and elemental composition of the formed bed particle layers. Ten typical bed particles and agglomerate necks (i.e., necks formed between bed particles) from each bed sample were analyzed. The elemental compositions were analyzed on the chosen particles with six spots (EDS) evenly distributed over the formed layers and agglomerate necks. Bed ash particles with sizes below 100 μm were sieved from the bed material samples taken at the end of the combustion period. The bed ash particle samples were then attached to carbon tape, and 15 elemental ash particles from each experiment were analyzed semiquantitatively by means of SEM/EDS. Bed material components and/or minerals introduced with the fuels, i.e., quartz (SiO_2), albite ($NaAlSi_3O_8$), and microcline ($KAlSi_3O_8$) grains were excluded during the analysis. The sieved bed ash samples were also analyzed with X-ray diffraction (XRD) for identification of crystalline phases. The XRD data collections were performed using a Bruker d8 Advance instrument in $\theta-\theta$ mode, with an optical configuration consisting of a primary Göbel mirror, Cu K_α radiation, and a Våntec-1 detector. Continuous scans were applied. By adding repeated scans, the total data collection time for each sample lasted for at least 6 h. The PDF2 databank[26] together with Bruker software was used to make initial qualitative identifications. The data were further analyzed with the Rietveld technique and data from ICSD[27] to obtain semiquantitative information of the present crystalline phases. The samples were subsequently analyzed by SEM/EDS, allowing for direct comparison of the two methods.

3. RESULTS

3.1. Initial Defluidization Temperatures in Controlled Bench-Scale Fluidized Bed Agglomeration Tests (CFBA). The results from the CFBA tests are listed in Table 3. Experiments with pure logging residues, bark, and RM showed relatively low bed agglomeration tendencies, i.e., the initial defluidization temperatures were well above the normal operational bed temperatures in FB values (800−900 °C) for these fuels. For the mixtures with 40 wt % DDGS in logging residues and both samples with phosphoric acid (PA) in logging residues, the defluidization temperatures were much lower compared to those of the pure fuel. The same tendencies were found for 30 wt % rapeseed meal in bark.

Pure DDGS and wheat straw fuels showed high bed agglomeration tendencies. Willow showed relatively moderate agglomeration tendency, while the mixture with 50 wt % DDGS in willow had significantly higher bed agglomeration tendency. Addition of DDGS (50 wt %) to wheat straw resulted also in an increased agglomeration tendency, while PA addition lowered it significantly.

3.2. Bed Particle Layer Characteristics. Combustion of logging residues, 40 wt % DDGS in logging residues, logging residues + PA-low, willow, and bark resulted in relatively continuous and homogeneous inner reaction layers and more granular structured outer coating layers on the bed particles. Typical bed particle cross sections for these fuels are shown in Figure 1. Only discontinuous (outer) coating layers resembling lumps of residual ash particles adhered to the bed particle grain surfaces during the combustion of DDGS, RM, 30 wt % rapeseed meal in bark, logging residues + PA-high, wheat straw, 50 wt % DDGS in wheat straw, wheat straw + PA, and 50 wt % DDGS in willow. Figure 2 shows some examples.

The elemental composition of the inner reaction layer for 40 wt % DDGS in logging residues was dominated by Si, K, and Mg, while for logging residues + PA-low, willow, and bark the

Table 2. Total Ash Content and the Content of Main Ash-forming Elements in the Produced Pellets Samples[a]

	40 wt % DDGS in logging residues	50 wt % DDGS in willow	50 wt % DDGS in wheat straw	logging residues + PA-low	logging residues + PA-high	wheat straw + PA	RM[b]	30 wt % rapeseed meal in bark[b]
ash	3.2	3.3	5.05	2.4	2.4	5.6	6.0	4.8
Si	0.21	0.094	0.45	0.29	0.29	0.79	0.08	0.38
Al	0.022	0.009	0.004	0.036	0.036	0.006	0.01	0.06
Ca	0.34	0.305	0.25	0.50	0.50	0.40	0.59	0.74
Fe	0.018	0.01	0.008	0.024	0.024	0.005	0.03	0.04
K	0.53	0.65	1.15	0.17	0.17	1.23	1.06	0.53
Mg	0.15	0.16	0.19	0.06	0.06	0.10	0.43	0.21
Na	0.012	0.011	0.02	0.014	0.014	0.03	0.01	0.03
P	0.36	0.44	0.48	0.068	0.12	0.50	1.01	0.40
S	0.404	0.5	0.57	0.04	0.04	0.19	0.73	0.30
Cl	<0.09	<0.10	0.24	<0.01	<0.01	0.26	0.02	0.023

[a] Values are calculated from the raw material compositions. Values given in weight percent of dry substance. [b] From Boström et al.[19]

Table 3. Initial Defluidization Temperatures for the Used Fuels

	temperature of initial defluidization (°C)	combustion time (h)
DDGS	total def. during comb. at ~800	1.5
RM[a]	1020	8
logging residues	1030	8
40 wt % DDGS in logging residues	950	8
logging residues + PA-low	980	8
logging residues + PA-high	990	8
bark	1050	8
30 wt % rapeseed meal in bark[a]	930	8
willow	900	8
50 wt % DDGS in willow	def. under comb. at ~800	7.5
wheat straw	750	8
50 wt % DDGS in wheat straw	total def. during comb. at ~730	2
wheat straw +PA	880	8

[a] From Boström et al. [16]

elemental composition of the inner reaction layer was dominated by Si, K, and Ca (Figure 3). The elemental composition for logging residues is not shown because the inner layers were too thin and the influence of the bed material on the results of the elemental analysis could not be excluded because of the limited spatial resolution for quantification with SEM/EDS (few micrometers). The outer coating layers for logging residues, logging residues + PA-low, willow, and bark, consisted mainly of Si, Ca, K, and minor amounts of Mg. In combustion of 40 wt % DDGS in logging residues, high content of P was found also in the outer coating layers (Figure 4).

The elemental composition of the (outer) coating layers for wheat straw was dominated by Si and K. For the mixtures with 50% DDGS and PA, the coating layers consisted mainly of Si, K, P, and minor amounts of Ca and Mg. Main coating layer elements for logging residues + PA-high, 50 wt % DDGS in willow, RM, and 30 wt % rapeseed meal in bark were Si, P, Ca, K, and Mg. In combustion of 30 wt % rapeseed meal in bark, Ca was found in high content, and for this fuel, S was found also in relatively high concentrations. Pure DDGS combustion resulted in P-, K-, Mg-, and Si-dominated coating layers (Figure 5).

3.3. Separate Bed Ash Particle Composition. Individual separate ash particles were also found in the bed samples in varied amounts depending on the fuel. The XRD analysis of the sieved bed samples showed the occurrence of minerals introduced as contaminants of the fuel, i.e., quartz (SiO_2), microcline ($KAlSi_3O_8$), and albite ($NaAlSi_3O_8$). The XRD results in Table 4 are therefore presented on a sand mineral-free basis in order to obtain comparable results. It should also be observed that the bed ash includes material that probably has been partially molten and that upon cooling formed mainly crystalline phases but also a fraction of amorphous material. The latter cannot be directly identified by XRD; thus, only indirect evidence of its existence is at hand obtained by comparing results from SEM/EDS and XRD analysis.

For willow and logging residues, the amounts of individual separate bed ash particles in the bed samples were low. For willow, no SEM/XRD analysis could be done because the ash particles retained in the bed were too scarce for analyzable amounts to be separated. The amount of separate bed ash particles found for both mixtures of logging residues + PA were higher than that for the pure fuel case. Detected crystalline phases were mainly Ca, Ca−K, and K−Mg phosphates and Ca−Mg silicates. In combustion of bark, slightly more individual ash particles were found in the bed, and detected crystalline phases were mainly Ca−Mg silicates, $Ca_5(PO_4)_3(OH)$, and $CaSO_4$. For wheat straw, DDGS, RM, wheat straw mixed with 50 wt % DDGS and PA, 50 wt % DDGS in willow, 40 wt % DDGS in logging

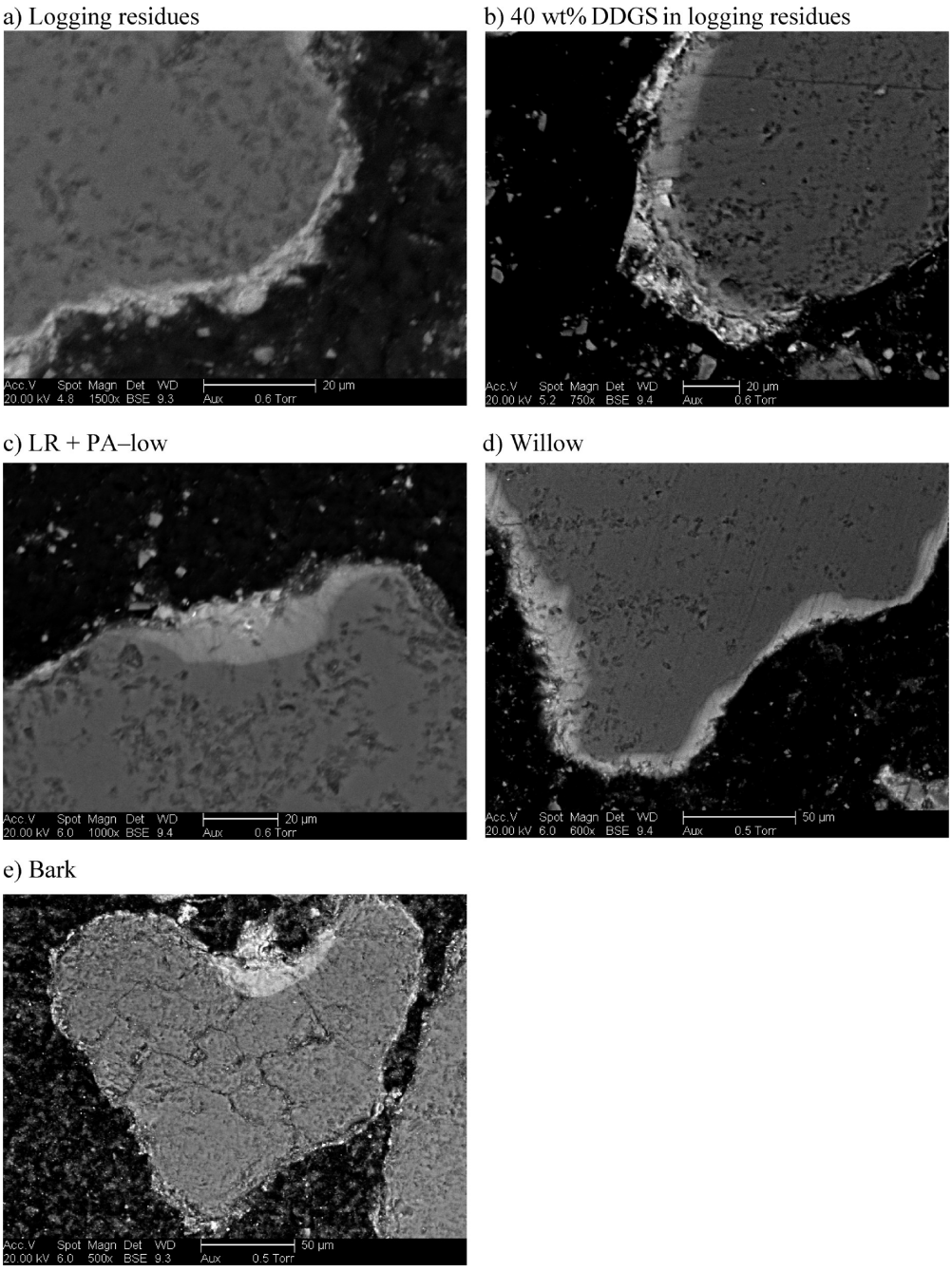

Figure 1. Scanning electron microscopy (SEM) images of typical cross sections of bed particle layers/coatings formed during combustion of logging residues, 40 wt % DDGS in logging residues, logging residues + PA-low, willow, and bark.

residues, and 30 wt % rapeseed in bark, the amount of individual ash particles in the bed samples were high, and for these fuels, detected crystalline phases were mainly Ca, Ca−K, and K−Mg phosphates, Ca−Mg silicates, and for some fuels, also cristobalite (SiO_2). The elemental compositions of the analyzed separate bed ash particles for all studied mixtures are shown in Figures 6 and 7 and resemble the coating/outer coating layers, except for slightly lower Si and higher P contents.

3.4. Agglomerate Neck Composition. The elemental composition of the agglomerate necks is shown in Figures 8 and 9. Agglomerate neck compositions are similar to the inner reaction bed particle layers for willow and bark. Wheat straw, DDGS, RM, and the fuel mixtures of wheat straw, logging residues, bark, and willow with the phosphorus-rich fuels/additives formed agglomerate necks that resembled the compositions of the discontinuous (outer) bed particle coating layers.

4. DISCUSSION

The following discussion is based on relative compositional differences and changes in the bed material and ash fractions as obtained from the SEM/EDS and the XRD analyses as well as on the result from the CFBA test. Table 5 summarizes the results presented in section 3.

Thermodynamical stability calculations under conditions relevant for the present combustion experiments and previous

dx.doi.org/10.1021/ef101451e |*Energy Fuels* 2011, 25, 937–947

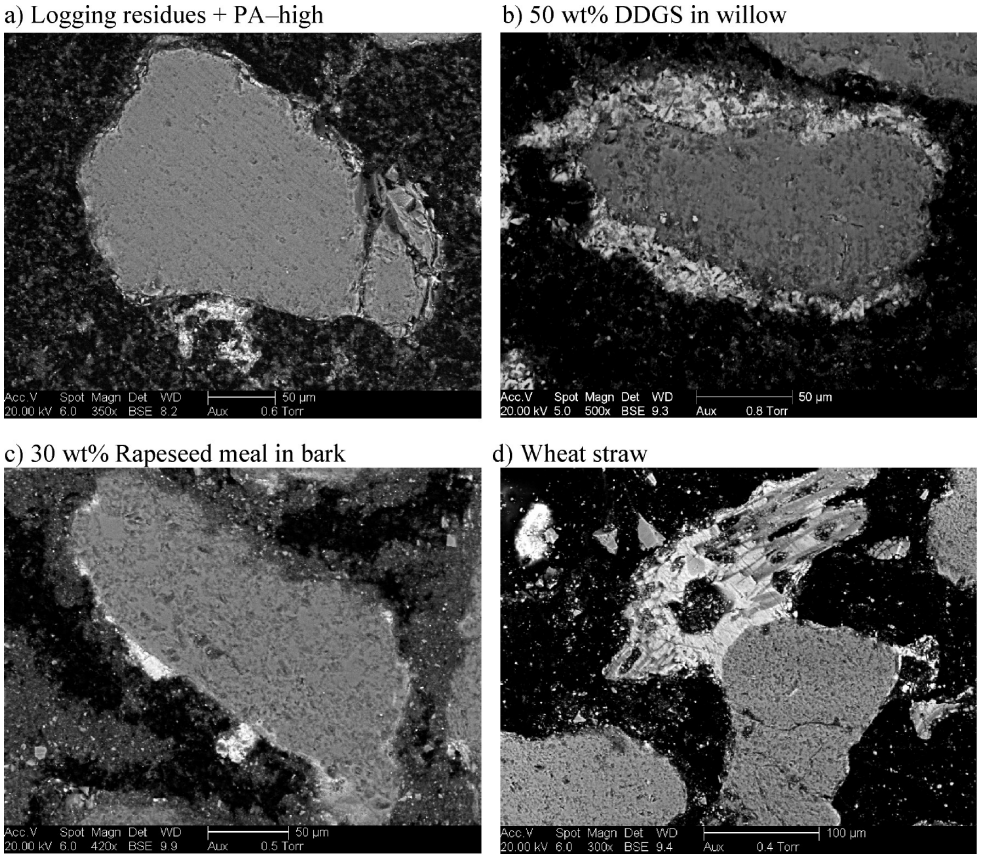

Figure 2. Scanning electron microscopy (SEM) images of typical cross sections of bed particle coating layers formed during the combustion of logging residues + PA-high, 50 wt % DDGS in willow, 30 wt % rapeseed meal in bark, and wheat straw.

research[18,19,28] have shown that P_2O_5 (g) dominates over SO_2/SO_3 (g), HCl (g), SiO_2 (g), and CO_2 (g) in the competition for the basic components, i.e., KOH (l,g), NaOH (l,g), CaO (s), and MgO (s). In a situation where there is a competition for P_2O_5 (g) among the basic cations, in ideal cases K phosphates are formed first, followed by Na, Ca, and Mg. If there is a competition for K among the acidic oxide components, K phosphates are formed first, followed by sulphates, chlorides, silicates, carbonates, and hydroxides. In real cases, ternary compounds such as, for instance, K−Ca phosphates and K−Mg phosphates are formed. Any unreacted or leftover organically bound Si may under such conditions form cristobalite or tridymite, i.e., different modifications of silica (SiO_2).

For logging residues, bark, and willow, which have relatively high Ca and K contents in comparison to P and organic bound Si, the inner reaction layer and agglomerate necks were found to have similar compositions dominated by Si, K, and Ca (Table 5); thus, mainly the inner layer is responsible for the bed agglomeration process. The layer formation is initiated by the reaction of gaseous or liquid K compounds with the surface of the bed particles to form a potassium silicate melt accompanied by diffusion/dissolving of Ca into the melt, followed by viscous flow sintering and agglomeration, according mechanism (a), as has been shown in previous studies.[6,7,14] The lower Ca/K ratio in the willow leads to higher agglomeration tendencies.

Wheat straw is a well-known problematic fuel, with an ash dominated by Si and K. Bed particles coating layers, agglomerate necks, and bed ash particles were all dominated by K and Si, (Table 5). Comparison of the results from XRD and SEM/EDS

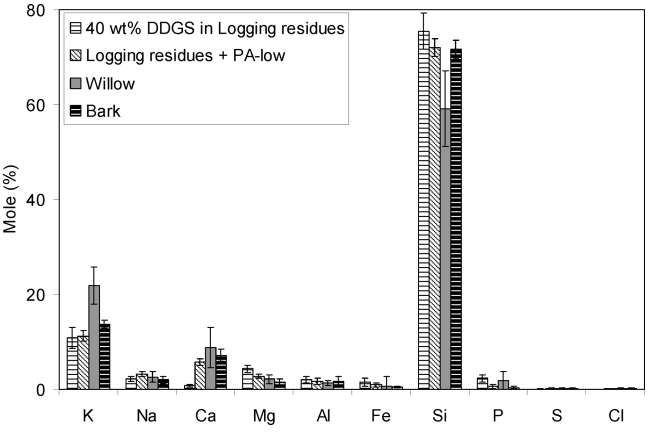

Figure 3. Elemental composition on C- and O-free basis of the inner reaction layers for 40 wt % DDGS in logging residues, logging residues + PA-low, willow, and bark.

analyses indicates that the organically bound Si mainly ends up in amorphous phases in the bed ash samples. Such partially molten alkali-rich silicate particles will occasionally stick to the bed particles forming noncontinuous layers, which subsequently will agglomerate, thus following mechanism (c), described as direct adhesion of the bed particles by partially molten ash K silicate ash particles. Similar results were also found in other works.[11,14,29]

For both mixtures of logging residues with phosphoric acid, PA-low, and PA-high, the only change in the composition

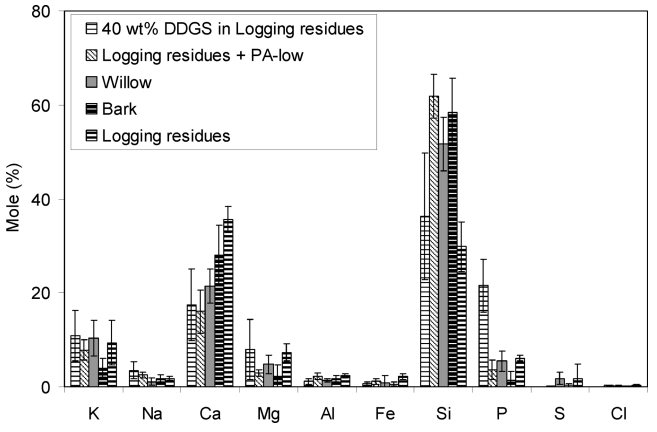

Figure 4. Elemental composition on C- and O-free basis of the outer coating layers for 40 wt % DDGS in logging residues, logging residues + PA-low, willow, bark, and logging residues.

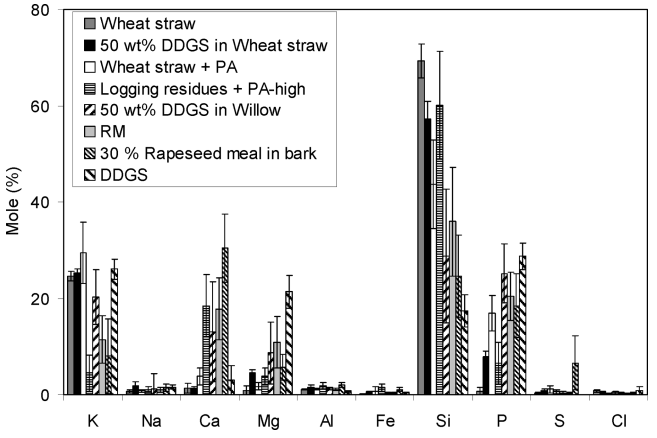

Figure 5. Elemental composition on C- and O-free basis of the (outer) coating layers for wheat straw, 50 wt % DDGS in wheat straw, wheat straw + PA, logging residues + PA-high, 50 wt % DDGS in willow, RM, 30 wt % rapeseed meal in bark, and DDGS.

compared to the pure fuel is that the P/K ratio is increased from 0.34 to 0.5 and 0.9, respectively. However, while in combustion of pure logging residues, the individual bed ash particles are dominated by silicates, and K−Ca−Mg phosphates are found in the bed ash in the presence of PA, which is in agreement with the thermodynamical stability calculations as previously mentioned. Compared to the pure logging residues, a difference in the combustion of the PA-low mixture was the presence of thick, continuous inner reaction layers rich in Si, K, and less amounts of Ca (Table 5 and Figure 1c). Thick noncontinuous (outer) coating layers containing Si, Ca, P, and K appeared when the P concentration in the mixture was increased to PA-high, while the inner reaction layer was absent (Table 5 and Figure 2a).

Our interpretation of the results from the PA-low mixture is that the available amount of P was not sufficient to eliminate the reaction of gaseous or liquid K compounds on the quartz bed grains, leading to K phosphate formation. Part of the alkali earth oxides will react together with the alkali phosphates to form more stable ternary phosphates, thus withdrawing some of those refractory components from dissolving into the K silicate layer on the bed grains.

In the PA-high mixture, the available amount of P appears to be enough to capture most of the K because no inner reaction layers were present on the quartz bed grains. Also a slight increase in Ca−K−Mg phosphate phases in the bed ash particles along with a decrease in Ca−Mg silicate phases were found compared to the PA-low mixture (Table 4). SEM analysis indicated that mainly the outer coating layer was involved in the bed agglomeration for both mixtures with PA, and the agglomeration tendency was increased compared to that of the pure fuel. Apparently, compared to the K−Ca-rich silicate inner reaction layer occurring in the pure fuel, the formation of a complex silicate−phosphate outer coating layer causes a lowering of the melting temperature. Unfortunately, no information concerning the melting behavior of such complex multicomponent mixtures are available.

DDGS and RM have similar fuel ash compositions, except for the Ca content which is about six times higher in the RM than in DDGS. Coating layers, agglomerate necks, and separate bed ash particles were found to resemble compositions dominated by P, K, Mg, and Si for DDGS and Si, P, Ca, Mg, and K for RM (Table 5). Although, the coating layers and agglomerate necks had higher Si concentrations than the separate bed ash particles probably because of reactions between the partially molten coating layer and the bed material grains. Significant amounts of bed ash particles were found in the bed for both fuels with a composition dominated by Ca−K−Mg phosphates. However, RM bed ash was enriched in Ca−Mg phosphates compared to that of DDGS (Table 4). An interpretation of the available K−Ca−P and K−Mg−P phase diagrams[17,30−36] indicate the formation of compounds with melting temperatures as low as 700 °C for KPO_3, while an increased content of Ca or Mg in the phosphates strongly shifts the melting temperatures to over 1000 °C. In DDGS, there are only small amounts of Ca and Mg that can be incorporated by the formed K-rich phosphate ash particles to increase their melting temperature. For the RM fuel, the K-rich phosphates incorporated noticeable amounts of CaO (s) yielding Ca-rich phosphate ash particles with melting temperatures over 1000 °C as found by XRD. This is the reason for the large difference in defluidization temperature between these P-rich fuels. Partially molten ash particles will occasionally adhere and react with the bed grains forming noncontinuous (outer) coatings layers and agglomerate necks with similar composition. The bed agglomeration mechanism can be then described as direct adhesion of bed particles by partially molten K−Mg phosphates for DDGS and partially molten K−Ca−Mg phosphates for RM.

The addition of 40 wt % DDGS to the logging residues (leading to P/K molar ratio 0.86) resulted in formation of thicker continuous inner reaction layers (than for the logging residue case) rich in Si, K, and Mg (Figure 1b and Table 5). Though the PA-high mixture has a similar P/K molar ratio (0.91), no inner layers were found in combustion of this mixture. This probably took place because of the much lower total K content; that is, the high amount of K introduced by the DDGS additive enhanced the reaction of gaseous or liquid K compounds on the quartz bed grains, leading to thick inner reaction layers. Bed particle outer coating layers, agglomerate necks, and bed ash particles had similar compositions, mainly K, Ca, Mg, P, and Si (Table 5). Becasue of the high K content in the fuel mixture, K phosphates are formed initially during combustion and will probably incorporate a part of the available Ca and Mg oxides forming compounds with lower melting temperatures than the Ca−Mg

dx.doi.org/10.1021/ef101451e |*Energy Fuels* 2011, 25, 937–947

Table 4. Crystalline Phases Identified with XRD in the Sieved Bed Samples[a]

	logging residues	bark	wheat straw	RM	DDGS	40 wt % DDGS in Logging residues	50 wt % DDGS in Willow	50 wt % DDGS in Wheat straw	logging residues + PA-low	logging residues + PA-high	wheat straw + PA	30 wt % rapeseed meal in bark
$CaCO_3$	11				14							
MgO						2						
$CaSO_4$		13			8	2			2	6		7
K_2SO_4	11		61	10	10			30			20	10
$K_3Na(SO_4)_2$			4					11				
KCl			3									
$Ca_5(PO_4)_3(OH)$	21	35	9					6				6
$Ca_3(PO_4)_2$				28	8	36	7		29	35		25
$CaK_2P_2O_7$				15	34	18	10	16	8	6	51	7
$CaKPO_4$			18								7	
$CaMgP_2O_7$										18		
$KMgPO_4$				35	12	27	16	14	23	13		30
$Ca_3Mg(SiO_4)_2$		35	2	6	14	15	18	11	18	13		6
$Ca_2MgSi_2O_7$		17	3	6			11	6	12	6		4
$CaMg(SiO_3)_2$	37						5					
SiO_2 (cristobalite)	20						33	6	4	3	22	3

[a] Values in the table give the contents of crystalline phases (wt %) on a sand mineral-free basis in the different samples as the result of semiquantitative refinement of the XRD data with Rietveld technique of the bed ashes. Results are shown in quartz (SiO_2)-, microcline ($KAlSi_3O_8$)-, and albite ($NaAlSi_3O_8$)-free basis. (Quantification for willow bed ash was not possible because of the scarce amount of sample).

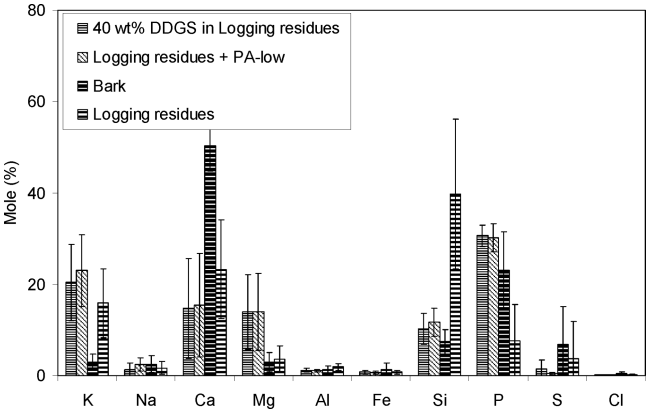

Figure 6. Elemental composition on C- and O-free basis of the separate bed ash particles found in the bed samples for 40 wt % DDGS in logging residues, logging residues + PA-low, bark, and logging residues.

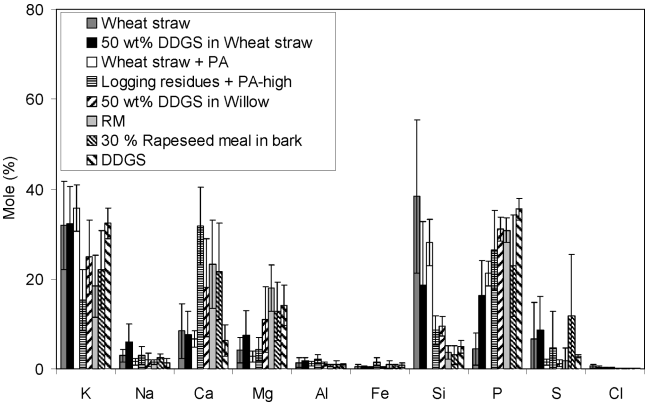

Figure 7. Elemental composition on C- and O-free basis of the separate bed ash particles found in the bed samples for wheat straw, 50 wt % DDGS in wheat straw, wheat straw + PA, logging residues + PA-high, 50 wt % DDGS in willow, RM, 30 wt % rapeseed meal in bark, and DDGS.

silicates formed in combustion of the pure logging residues. The SEM analysis of the bed material and agglomerates shows that the outer coating layer was responsible for the bed agglomeration process. Partially molten ash particles consisting of K−Ca−Mg phosphates will occasionally adhere to and react with the bed particles and form noncontinuous layers and agglomerates.

In the mixture of 30 wt % rapeseed meal with bark, the molar P/K ratio is increased from 0.24 for bark to 0.96. The (outer) coating layers, agglomerate necks, and the bed ash have relatively similar elemental compositions dominated by K, Ca, Mg, Si, P, and S (Table 5). The coating layers here also had higher Si concentrations than the separate bed ash particles, probably because of reactions between the partially molten coating layer and the bed material grains. Similarly to the logging residue mixtures, the amount of introduced P determines the ash formation behavior. SEM analysis of the bed material shows that mainly the (outer) coating layer was responsible for the bed agglomeration process. During the combustion of the rapeseed meal mixture, K phosphates are initially formed, subsequently incorporating Ca and Mg oxides. Sulfur oxides react with the remaining unreacted basic oxides forming Ca and K sulphates. The ability of P and S to act as K-capturing agents was efficient enough to reduce the concentration of gaseous or liquid K species to very low levels because no inner reaction layers rich in K were found, while cristobalite (SiO_2) was detected in the separate bed ash particles, thus indicating that some of the fuel-bound Si did not react further from the formation of silica. The ash particles containing K−Ca−Mg phosphates that probably

dx.doi.org/10.1021/ef101451e |*Energy Fuels* 2011, 25, 937–947

interacted with Ca −sulphates will occasionally stick to the bed particles forming noncontinuous layers and agglomerates.

In the mixture of 50 wt % DDGS in wheat straw, the K content does not change much compared to the pure fuels. The Si and P contents approach similar levels, while the Ca content decreases and Mg increases, although the sum of these basic components is almost constant. This means blending a low melting K−Si-dominated fuel (wheat straw) with a low melting K−P-dominated fuel (DDGS) to a fuel mixture that promotes the formation of low-temperature K−Ca−Mg phosphate/silicate melts. SEM analysis showed that molten ash/(outer) coating layer was the main factor responsible for the bed agglomeration. Agglomerate necks and coating layers show similar elemental composition with the main elements being K, Si, and P (Table 5). The crystalline phases in the bed ash are dominated by Ca−K−Mg phosphates, Ca−Mg silicates, K−Na sulphates, and cristobalite (SiO_2), indicating that some of the organically bound Si did not react with K to form K silicates. Apparently, compared to the K-rich silicate (outer) coating layer occurring in the pure wheat fuel, the formation of a complex silicate−phosphate outer coating layer causes a lowering of the melting temperature. Partially molten ash particles will occasionally stick to the bed particles forming noncontinuous layers and subsequently agglomerates, following the agglomeration mechanism described for this fuel as direct adhesion of bed particles by partially molten K−Ca−Mg phosphates/silicates.

For the mixture of wheat straw + PA, the only change in the fuel composition is an increase in the P content, promoting K−Ca phosphate formation in the bed. $CaK_2P_2O_7$ and $CaKPO_4$ were found in the individual bed ash particles together with K_2SO_4 and cristobalite (SiO_2). Agglomerate necks and outer coating layers are mainly composed of Si, K, and P (Table 5). During combustion, the P in the fuel mixture reacts with K, forming K-rich phosphates that subsequently react further with CaO(s), resulting in decreased formation of low melting

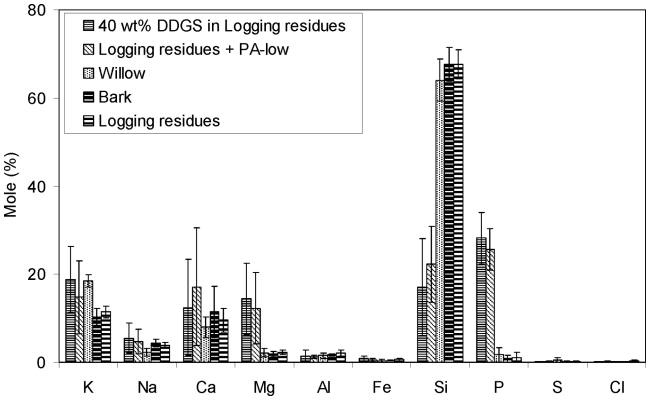

Figure 8. Elemental composition on C-and O-free basis of the agglomerate necks for 40 wt % DDGS in logging residues, logging residues + PA-low, willow, bark, and logging residues.

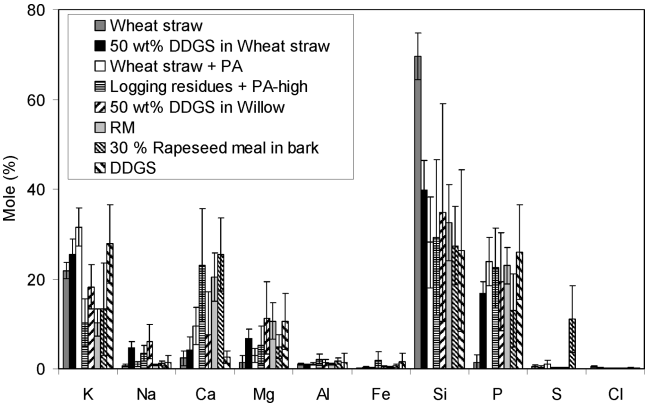

Figure 9. Elemental composition on C- and O-free basis of the agglomerate necks for wheat straw, 50 wt % DDGS in wheat straw, wheat straw + PA, logging residues + PA-high, 50 wt % DDGS in willow, RM, 30 wt % rapeseed meal in bark, and DDGS.

Table 5. Summary of the Results: Fuel Characteristics (P/K and P/Ca + Mg Molar Ratio), Dominating Elements in Inner Bed Particle Reaction Layers, (Outer) Bed Particle Coating Layers, Agglomerate Necks, Individual Bed Ash Particles from the SEM/EDS Analysis, and Initial Defluidization Temperature According to CFBA Experiments

fuel	P/K[a]	P/Ca + Mg[a]	dominating[b] inner reaction layer elements	dominating[b] coating layer elements	dominating[b] neck elements	dominating[b] bed ash particles elements	CFBA initial defluidization temperature (°C)
logging residues	0.34	0.10	(too thin)	Ca, Si, K, Mg	Si, K, Ca	small amounts	1030
bark	0.25	0.06	Si, K, Ca	Si, Ca, K, Mg	Si, Ca, K	small amounts	1050
willow	0.30	0.13	Si, K, Ca	Si, Ca, K, Mg	Si, K, Ca	n.d	900
wheat straw	0.13	0.30	−	Si, K	Si, K	Si, K, Ca	750
RM	1.2	1.0	−	Si, P, Ca, Mg, K	Si, P, Ca, Mg, K	P, Ca, K, Mg, Si	1020
DDGS	0.98	2.0	−	P, K, Mg, Si	Si, P, K, Mg	P, K, Mg, Si	total defl. at ∼800
40 wt % DDGS in logging residues	0.86	0.80	Si, K, Mg	Si, P, Ca, K, Mg	P, Si, K, Mg, Ca	P, K, Ca, Mg, Si	950
logging residues + PA-low	0.50	0.15	Si, K, Ca	Si, Ca, K, Mg, P	P, Si, Ca, K, Mg	P, K, Ca, Mg, Si	980
logging residues + PA-high	0.91	0.27	−	Si, Ca, P, K	Si, P, Ca, K	Ca, P, K, Si	990
30 wt % rapeseed meal in bark	0.96	0.50	−	Ca, Si, P, K, S	Si, Ca, P, K, S	P, K, Ca, Mg, S	930
50 wt % DDGS in wheat straw	0.52	1.0	−	Si, K, P	Si, K, P	K, Si, P, Ca, Mg	total defl. at ∼730
wheat straw + PA	0.51	1.15	−	Si, K, P	K, Si, P	K, Si, P, Ca	880
50 wt % DDGS in willow	0.85	1.0	−	Si, P, K, Ca, Mg	Si, P, K, Mg	P, K, Ca, Mg, Si	defl. at ∼800

[a] Fuel ash P/K and P/Ca + Mg molar ratio. [b] Concentrations > ∼5 mol % on an O- and C-free basis. Compositions are found in Figures 3 − 9. Elements in the table are ordered in decreasing concentration from left to right.

dx.doi.org/10.1021/ef101451e |*Energy Fuels* 2011, 25, 937–947

temperature silicates because less K is available for reaction with the organically bound Si, yielding cristobalite (SiO_2) in the bed ash as a result (Table 4). That is, shifting the fuel composition to a higher P content resulted in an ash system with melting temperatures higher than those in the K−silicate-dominated ash system found for the pure wheat straw. When comparing the mixtures of wheat straw + PA and 50 wt % DDGS, in the latter two, low melting ash systems (K−Si-dominated and K−P-dominated) are mixed, which leads to a mixture with melting temperatures lower than both ash systems separately (Table 3), while, in the mixture with PA, part of the low melting temperature K silicates are "replaced" by more stable Ca−K phosphates, leading to significantly increased initial defluidization temperatures greater than 120 °C (Table 5). However, it seems that the P increase through the additive was not large enough because ash particles and agglomerate necks rich in K, P, and Si, probably as amorphous K−silicates phosphates, were still found. The agglomeration for this fuel can be described as direct adhesion of bed particles by partially molten K−Ca phosphates/silicates.

The mixture of 50 wt % DDGS with willow contains high amounts of K introduced with the DDGS. While the P/K ratio is 0.85, the contents of Ca, Mg, and Si are relatively low. Main elements in the outer coating layers, necks, and bed ash are P, K, Ca, Mg, and Si (Table 5). The individual bed ash particles are dominated by Ca−K−Mg phosphates and Ca−Mg silicates. Similarly to other mixtures, K and P in the fuel mixture will react during combustion and form K phosphates that subsequently react further with Ca and Mg oxides, increasing the melting temperature of the bed ash K-rich phosphates. This effect is, however, not large enough considering the high amounts of K supplied by the DDGS; thus, the resulting K−Ca−Mg phosphates mixture will still be rich in K with probably relatively low melting temperatures. Hence, even though K does not react to any large extent with quartz bed grains forming low melting K silicates, the defluidization temperature is still lower than that for willow (Table 5). Compared to the K-rich silicate inner reaction layer occurring for the pure willow, partially molten ash particles will adhere and react with the bed grains to form noncontinuous complex silicate−phosphate coatings on the bed grains. This follows the agglomeration mechanism described as agglomeration induced by partially molten K−Ca−Mg silicates/phosphates.

5. CONCLUSIONS

- In combustion of logging residues, bark, and willow (with ash relatively rich in K and Ca in comparison to P and organically bound Si), the bed layer formation was initiated by a potassium silicate melt formed on the quartz bed particles surface, a result of the gaseous or liquid K compounds reaction with the bed material. This process was accompanied by diffusion/dissolving of Ca into the melt, followed by viscous flow sintering and agglomeration.
- Addition of high enough phosphorus to the wood-derived fuels (through cocombustion with P-rich fuels or additives) converted the available fuel ash basic oxides K, Ca, and Mg into phosphates. Therefore, it reduced the amount of K available for the reaction with the quartz bed material grains. The phosphate-rich ash particles that are partially molten may adhere and react with the bed material grains forming noncontinuous silicate/phosphate coating layers that are responsible for the agglomeration process. The fuels rich in phosphorus (RM and DDGS) with a composition similar to the woody fuels mixed with additives display similar bed agglomeration characteristics.
- For the wheat straw (fuel ash dominated by Si and K), partially molten alkali-rich silicate ash particles were formed during combustion and adhered to the bed particles forming noncontinuous layers and subsequently agglomerates. Increasing the phosphorus content in the pure wheat straw (by cofiring with P-rich fuels or additives) lead to the formation of partially molten alkali-rich silicate/phosphate ash particles that also adhered to the bed particles causing agglomeration.
- The melting behavior of the bed particle layers/coatings is an important controlling factor behind the agglomeration tendency. For combustion of phosphorus-rich fuels and fuel mixtures, the melting is heavily dependent on the content of the alkaline earth metals in the fuel.
- A general observation is that phosphorus is the controlling element in the ash transformation reactions during biomass combustion in fluidized quartz beds because of the high stability of phosphate compounds.

AUTHOR INFORMATION

Corresponding Author
*Phone: +46 (0)920 491237. E-mail: Alejandro.Grimm@ltu.se.

ACKNOWLEDGMENT

The financial support from the Swedish Research Council (VR) is gratefully acknowledged. For the valuable help and comments on the manuscript, Associate Professor Emilia Björnbom (Department of Chemical Engineering and Technology, Royal Institute of Technology, Stockholm) is also gratefully acknowledged. The authors also thank Patrycja Piotrowska (Process Chemistry Centre, Åbo Akademi University), for the comments on the manuscript. The support given by Ulf Nordström (Energy Technology and Thermal Process Chemistry, Umeå University), during the experiments is gratefully appreciated.

REFERENCES

(1) Khan, A. A.; De Jong, W.; Jansens, P. J.; Spliethoff, H. *Fuel Process. Technol.* **2009**, *90*, 21–50.
(2) Brus, E. *Bed Agglomeration during Combustion and Gasification of Biomass Fuels: Mechanisms and Measures for Prevention*. Licenciate Thesis, Umeå University, Umeå, 2004, ISBN 91-7305-676-6.
(3) Zevenhoven-Onderwater. *Ash-Forming Matter in Biomass Fuels*. Academic Dissertation, Report 01-03, Åbo Akademi, Finland, 2000.
(4) Werther, J.; Saenger, M.; Hartge, E. U.; Ogada, T.; Siagi, Z. *Prog. Energy Combust. Sci.* **2000**, *26*, 1–27.
(5) Bartels, M.; Lin, W.; Nijenhuis, J.; Kapteijn, F.; Ruud van Ommen, J. *Prog. Energy Combust. Sci.* **2008**, *34*, 633–666.
(6) De Geyter, S.; Öhman, M.; Boström, D.; Eriksson, M.; Nordin, A. *Energy Fuels* **2007**, *21*, 2663–2668.
(7) Öhman, M.; Pommer, L.; Nordin, A. *Energy Fuels* **2005**, *19*, 1742–1748.
(8) Anthony, E. J. *Prog. Energy Combust. Sci.* **1995**, *21*, 239–268.
(9) Werther, J.; Saenger, M.; Hartge, E. U.; Ogada, T.; Siagi, Z. *Prog. Energy Combust. Sci.* **2000**, *26*, 1–27.
(10) Brus, E.; Öhman, M.; Nordin, A. *Energy Fuels* **2005**, *19*, 825–832.
(11) Öhman, M.; Nordin, A.; Skrifvars, B.−J.; Backman, R.; Hupa, M. *Energy Fuels* **2000**, *14*, 169–178.

(12) Latva−Somppi, J.; Kauppinen, E. I.; Valmari, T.; Ahonen, P.; Burav, A. S.; Kodas, T. T.; Johanson, B. *Fuel Process. Technol.* **1998**, *54*, 79–94.
(13) Nuutinen, L. H.; Tiainen, M. S.; Virtanen, M. E.; Enestam, S. H.; Laitinen, R. S. *Energy Fuels* **2004**, *18* (1), 127–139.
(14) Brus, E.; Öhman, M.; Nordin, A.; Boström, D. *Energy Fuels* **2004**, *18*, 1187–1193.
(15) De Geyter, S. *Measures for Preventing Bed Agglomeration Using Ash Reaction Chemistry*. Licenciate Thesis, Umeå University, Umeå, 2008, ISBN 978-91-7264-707-7.
(16) Eriksson, G.; Hedman, H.; Boström, D.; Pettersson, E.; Backman, R.; Öhman, M. *Energy Fuels* **2009**, *23*, 3930–3939.
(17) Lindström, E.; Sandström, M.; Boström, D.; Öhman, M. *Energy Fuels* **2007**, *21*, 710–717.
(18) Boström, D.; Grimm, A.; Boman, C.; Björnbom, E.; Öhman, M. *Energy Fuels* **2009**, *23*, 5184–5190.
(19) Boström, D.; Eriksson, G.; Boman, C.; Öhman, M. *Energy Fuels* **2009**, *23*, 2700–2706.
(20) Piotrowska, P.; Zevenhoven, M.; Davidsson, D.; Hupa, M.; Åmand, L. E.; Barisié, V.; Coda Zabetta, E. *Energy Fuels* **2010**, *24*, 333–345.
(21) Barišić, V.; Åmand, L. E.; Coda Zabetta, E. *The Role of Limestone in Preventing Agglomeration and Slagging during Cfb Combustion of High-Phosphorous Fuels*; World Bioenergy: Jönköping, Sweden, **2008**.
(22) Silvennoinen, J.; Hedman M. Fluidized Bed Combustion of Agricultural Fuels Results of the Full-Scale Demonstration. Impacts of Fuel Quality on Power Production & Environment, Finland, August 29−September 3, **2010**.
(23) Fryda, L.; Panopoulos, K.; Vourliotis, P.; Pavlidou, E.; Kakaras, E. *Fuel* **2006**, *85*, 1685–1699.
(24) Shao, J.; Ho Lee, D.; Yan, R.; Liu, M.; Wang, X.; Tee Liang, D.; John White, T.; Chen, H. *Energy Fuels* **2007**, *21*, 2608–2614.
(25) Öhman, M.; Nordin, A. *Energy Fuels* **1998**, *12*, 90–94.
(26) *The Powder Diffraction File, PDF-2*; International Center for Diffraction Data: Newtown Square, PA, 2004.
(27) *Inorganic Crystal Structure Database (ICSD)*; National Institute of Standards and Technology, Fachinformationzentrum Karlsruhe: Karlsruhe, Germany.
(28) Boström, D.; Broström, M.; Skoglund, N.; Boman, C.; Backman, R.; Öhman, M.; Grimm, A. Ash Transformation Chemistry during Energy Conversion of Biomass. Impacts of Fuel Quality on Power Production & Environment, Finland, August 29− September 3, **2010**.
(29) Lin, W.; Dam-Johansen, K.; Frandsen, F. *Chem. Eng. J.* **2003**, *96*, 171–185.
(30) Novakovic, A.; Van Lith, S. C.; Frandsen, F. J.; Jensen, P. A.; Holgersen, L. B. *Energy Fuels* **2009**, *23*, 3423–3428.
(31) Sandström, M.; Boström, D.; Nordin, A. In Phases of Relevance for Ash Formation during Thermal Processing of Biomass and Sludges: Review of Thermodynamic Data, Phase Transition and Crystal Structures in the System $CaO-K_2O-P_2O_5$, 2nd World Biomass Conference and Exhibition, Rome, Italy, May 10−14, 2004.
(32) Znamierowska−Kubicka, T. Rocz. *Chem.* **1977**, *51* (11), 2089–2098.
(33) Znamierowska, T. *Pol. J. Chem.* **1978**, *52* (6), 1127–1134.
(34) Znamierowska, T. *Pol. J. Chem.* **1978**, *52* (10), 1889–1895.
(35) Znamierowska, T. *Pol. J. Chem.* **1979**, *53* (7−8), 1415–1423.
(36) Znamierowska, T. *Pol. J. Chem.* **1981**, *55* (4), 747–756.